Nebulization of PEGylated recombinant human deoxyribonuclease I using vibrating membrane nebulizers

Mahri, Sohaib; Wilms, Tobias; Hagedorm, Paul; Guichard, Marie Julie; Vanvarenberg, Kevin; Dumoulin, Mireille; Frijlink, Henderik; Vanbever, Rita

Published in:
European Journal of Pharmaceutical Sciences

DOI:
10.1016/j.ejps.2023.106522

Publication date:
2023

European Journal of Pharmaceutical Sciences 189 (2023) 106522

Contents lists available at ScienceDirect

European Journal of Pharmaceutical Sciences

journal homepage: www.elsevier.com/locate/ejps

Nebulization of PEGylated recombinant human deoxyribonuclease I using vibrating membrane nebulizers: A technical feasibility study

Sohaib Mahri [a], Tobias Wilms [a], Paul Hagedorm [b], Marie-Julie Guichard [a], Kevin Vanvarenberg [a], Mireille Dumoulin [c], Henderik Frijlink [b], Rita Vanbever [a,*]

[a] Université catholique de Louvain (UCLouvain), Louvain Drug Research Institute, Advanced Drug Delivery and Biomaterials, Brussels, Belgium
[b] University of Groningen, Groningen Research Institute of Pharmacy, Pharmaceutical Technology and Biopharmacy, Groningen, the Netherlands
[c] University of Liège, Center for Protein Engineering, InBioS, Nanobodies to Explore Protein Structure and Functions, Liège, Belgium

ARTICLE INFO

Keywords:
Recombinant human deoxyribonuclease I (rhDNase)
PEGylation
Cystic fibrosis
Thermodynamic stability
Vibrating mesh nebulization
Electrospraying

ABSTRACT

Recombinant human deoxyribonuclease I (rhDNase, Pulmozyme®) is the most frequently used mucolytic agent for the symptomatic treatment of cystic fibrosis (CF) lung disease. Conjugation of rhDNase to polyethylene glycol (PEG) has been shown to greatly prolong its residence time in the lungs and improve its therapeutic efficacy in mice. To present an added value over current rhDNase treatment, PEGylated rhDNase needs to be efficiently and less frequently administrated by aerosolization and possibly at higher concentrations than existing rhDNase. In this study, the effects of PEGylation on the thermodynamic stability of rhDNase was investigated using linear 20 kDa, linear 30 kDa and 2-armed 40 kDa PEGs. The suitability of PEG30-rhDNase to electrohydrodynamic atomization (electrospraying) as well as the feasibility of using two vibrating mesh nebulizers, the optimized eFlow® Technology nebulizer (eFlow) and Innospire Go, at varying protein concentrations were investigated. PEGylation was shown to destabilize rhDNase upon chemical-induced denaturation and ethanol exposure. Yet, PEG30-rhDNase was stable enough to withstand aerosolization stresses using the eFlow and Innospire Go nebulizers even at higher concentrations (5 mg of protein per ml) than conventional rhDNase formulation (1 mg/ml). High aerosol output (up to 1.5 ml per min) and excellent aerosol characteristics (up to 83% fine particle fraction) were achieved while preserving protein integrity and enzymatic activity. This work demonstrates the technical feasibility of PEG-rhDNase nebulization with advanced vibrating membrane nebulizers, encouraging further pharmaceutical and clinical developments of a long-acting PEGylated alternative to rhDNase for treating patients with CF.

1. Introduction

Recombinant human deoxyribonuclease I (rhDNase, Pulmozyme®) is the most frequently used mucolytic agent for the symptomatic treatment of the respiratory pathology in cystic fibrosis (CF). CF is a rare and serious genetic disease that affects around 100,000 people worldwide (Suri, 2005). It is a multi-systemic disease, affecting mainly the respiratory system, and this impairment is the leading cause of morbidity and mortality of the disease. Loss of function of the Cystic Fibrosis Transmembrane Conduct Regulator (CFTR) protein, a transcellular transporter of chloride ions, leads to obstruction of the airways with viscous secretions, thereby creating an ideal environment for the development of bacterial infections (Ratjen, 2009, Lubamba et al., 2012). Despite the recent development of highly effective

Abbreviations: bFGF, basic fibroblast growth factor; CF, cystic fibrosis; Cm, GdmCl-concentration at the mid-point of the unfolding transition; FPF, fine particle fraction; GdmCl, guanidinium chloride; GSD, geometric standard deviation; $\Delta G^{\circ}_{NU}(H_2O)$, difference in free energy between the folded (N) and unfolded (U) state; λmax, the wavelength corresponding to the highest fluorescence intensity; *m*, measure of the dependence of the free energy on the denaturant concentration; MG, methyl green; MMAD, mass median aerodynamic diameter; N, native state; PEG, polyethylene glycol; PEG20, linear 20 kDa polyethylene glycol; PEG30, linear 30 kDa polyethylene glycol; PEG40, two-armed 40 kDa polyethylene glycol; rhDNase, recombinant human deoxyribonuclease I; RT, room temperature; SEC, size exclusion chromatography; SEM, standard error of the mean; Tm, temperature of mid-transition; U, Unfolded state; VMD, Volume Median Diameter.

* Corresponding author at: Advanced Drug Delivery & Biomaterials, Louvain Drug Research Institute, Université Catholique de Louvain, Avenue E. Mounier, 73 Box B1.73.12, 1200, Brussels, Belgium.
E-mail address: rita.vanbever@uclouvain.be (R. Vanbever).

https://doi.org/10.1016/j.ejps.2023.106522
Received 9 February 2023; Received in revised form 16 June 2023; Accepted 6 July 2023
Available online 8 July 2023

next-generation CFTR modulator therapies, there is currently no curative treatment available. Fortunately, symptomatic treatment has played a pivotal role in increasing the life expectancy of patients affected by the disease. Although effective, this symptomatic treatment is costly and burdensome for patients because it requires more than two to three hours of treatment per day (Nasr et al., 2013). Therefore, a high unmet need to ease the therapy burden of patients with CF exists.

Pulmozyme® administration significantly contributes to the treatment burden of CF as it requires to be taken once or twice a day via nebulization lasting 10-15 minutes for each session. Therefore, Pulmozyme® treatment is associated with low patient adherence (50-60%) (Nasr et al., 2013). Low treatment adherence in CF has been shown to be associated with more frequent hospitalizations, higher healthcare costs and a decreased quality of life (Kettler et al., 2002). A promising strategy to improve patients' adherence could be to develop a long-acting PEGylated version of Pulmozyme® e.g., to be administered weekly, via a customized highly efficient mesh nebulizer. Indeed, PEGylation of rhDNase does not alter its enzymatic activity and prolongs its residence time and mucolytic action in the lungs of mice from a few hours (native rhDNase) to more than 14 days (Guichard et al., 2021). In addition, a one-week therapeutic efficacy study in β-ENaC mice, a murine model of the respiratory pathology in CF, showed that a single dose of PEG-rhDNase was as effective as daily administration of the same dose of unconjugated rhDNase over 5 consecutive days (Guichard et al., 2021).

PEGylation of proteins is not a novel technology as it has been widely used by the pharmaceutical industry to increase the plasma half-life of therapeutic proteins (Ekladious et al., 2019, Rondon et al., 2021). Currently, about 20 PEGylated drugs for injection are on the market and around 40 are in clinical development (Rondon et al., 2021). It is therefore a well-established technology in terms of efficacy and safety. However, no PEGylated therapeutic agent is currently approved by medicines regulatory agencies for pulmonary administration. In this context, it is noteworthy that the pharmaceutical company Bayer initiated a phase 2 clinical trial to test the safety and efficacy of an inhaled PEGylated peptide, i.e., adrenomedullin, to treat patients suffering from Acute Respiratory Distress Syndrome (NCT04417036). Still, very few PEGylated proteins are currently being studied for administration by the inhalation route, apart from PEG-rhDNase and PEG-alpha-1 antitrypsin (Guichard et al., 2021, Liu et al., 2022, Guichard et al., 2017).

Currently, rhDNase is delivered to the lungs solely through nebulization and so is most of inhaled protein therapeutics currently under development (Hertel et al., 2015, Bodier-Montagutelli et al., 2018). Several nebulization technologies such as jet, ultrasonic and vibrating-mesh nebulization have been investigated for protein delivery (Niven et al., 1994, Niven et al., 1995, Cipolla et al., 1994, Niven et al., 1996, Respaud et al., 2014, Respaud et al., 2016). Nebulization is notoriously stressful to proteins primarily due to physical stresses during the atomization step such as the generation of large air-liquid interface, evaporation, aerosol recirculation and heating (Hertel et al., 2015, Bodier-Montagutelli et al., 2020). Partial or total loss of biological activity commonly associated with physicochemical alterations such as degradation and/or aggregation may lead to a loss of efficacy and cause side effects as a result of the immunogenicity of degradation products.

Among nebulizers, the jet nebulizer has gained a historic relevance for being the first nebulizer approved by the FDA for rhDNase (Fuchs et al., 1994). Mesh nebulization, generally regarded as gentler for proteins, was shown to preserve the structural and enzymatic integrity of rhDNase and subsequently validated for rhDNase delivery unlike some ultrasonic nebulizers which easily cause protein denaturation (Cipolla et al., 1994, Johnson et al., 2008). Hydroelectrodynamic atomization is under development for inhalation (Gomez, 2002). Its advantage is the generation of a highly mono-dispersed aerosol which potentially offers high fine particle fractions and an ability to target specific lung regions. These are significant benefits for rhDNase as its preferential delivery to small airways has been shown to improve lung function in children with stable CF (Bakker et al., 2011).

Our team previously showed that PEGylated rhDNase with PEG30 kDa is stable to jet nebulization at a concentration akin to that used for the commercial rhDNase (1 mg/ml) (Guichard et al., 2021). However, for the purpose of achieving a faster and more efficient delivery, novel inhaler devices and higher protein concentrations were considered in this work. To gain more fundamental knowledge on the impact of PEGylation on the stability of rhDNase, the thermodynamic stability of rhDNase and its conjugates was evaluated. For that purpose, rhDNase conjugated to linear 20 kDa, linear 30 kDa or 2-armed 40 kDa PEG were exposed to increasing concentrations of guanidinium chloride (GdmCl), a denaturing agent, and the changes in the protein tertiary structure was monitored by intrinsic fluorescence. PEG30-rhDNase was further selected to carry on stability studies in high concentrations of ethanol to inform on the suitability of using hydroelectrodynamic atomization. The compatibility of PEG30-rhDNase with two vibrating mesh nebulizers, an optimized eFlow® Technology nebulizer (eFlow) (PARI) and InnoSpire Go (Philips), was also investigated. Aerosols generated by these devices were characterized by laser diffraction. Physicochemical stability of PEG30-rhDNase to nebulization was also assessed, focusing on the enzymatic activity and aggregates formation. Whenever available, data were compared to rhDNase reference formulation in the literature.

2. Material and Methods

2.1. Material

Recombinant human deoxyribonuclease I (rhDNase, Pulmozyme®) was purchased from Roche (Brussels, Belgium). Linear 20 kDa and 30 kDa and two-arm 40 kDa methoxy PEG propionaldehyde (PEG20, PEG30, and PEG40 respectively) were purchased from NOF Corporation (Tokyo, Japan). Resource Q 1 ml and HiLoad 16/60 superdex 200 columns were obtained from GE Healthcare (Bio-Sciences AB, Uppsala, Sweden). Superose® 6 Increase 10/300 GL and Superdex 75 Increase 10/300 GL column were obtained from Cytiva (Belgium). Ultrapure guanidinium chloride (GdmCl) was purchased from Sigma-Aldrich (St. Louis, MO, USA). Unless otherwise mentioned, other chemicals were purchased from Sigma-Aldrich (St. Louis, MO, USA).

2.2. PEGylation of rhDNase

Production of PEG20-rhDNase, PEG30-rhDNase, and PEG40-rhDNase was achieved by covalently attaching linear 20 kDa, linear 30 kDa or two-arm 40 kDa methoxy PEG propionaldehyde to the N-terminus of rhDNase (Guichard et al., 2017, Mahri et al., 2021). Briefly, commercial rhDNase (Pulmozyme®, 1 mg/ml in 150 mM NaCl, 1 mM $CaCl_2$) was concentrated to 5-10 mg/ml in 1 mM $CaCl_2$, 100 mM CH_3CO_2Na (sodium acetate buffer, pH 5) by ultrafiltration using vivaspin® Turbo 4, 3 kDa (Sartorius; Stonehouse, Gloucestershire, UK) then added to PEG propionaldehyde at a molar ratio PEG:rhDNase of 4:1 in the presence of 34 mM reducing agent $NaBH_3CN$. The reaction mixtures were stirred at room temperature overnight. Mono-PEGylated products were purified on ÄKTA™ purifier 10 system by anion exchange chromatography (Resource Q, 1 ml column) followed by size exclusion chromatography (SEC) on HiLoad 16/60 superdex 200 column (GE Healthcare Bio-Sciences AB, Uppsala, Sweden). PEGylated rhDNase products were filtered through 0.22 µm PVDF membranes and stored at 4°C in 150 mM NaCl, 1 mM $CaCl_2$, the storage buffer of Pulmozyme®.

2.3. Thermodynamic stability

2.3.1. Guanidinium chloride (GdmCl)-induced unfolding

rhDNase and PEGylated rhDNases (0.125 mg/mL of rhDNase, without counting the PEG mass in the concentration) were incubated in 150 mM NaCl, 1mM $CaCl_2$ containing GdmCl concentrations ranging from 0 to 5.1 M. Denaturant concentration in the samples were determined from refractive index measurements (Nozaki, 1972) using a

R5000 hand-held refractometer (Atago, Tokyo, Japan). The proteins were incubated overnight at 25°C and then intrinsic fluorescence spectra were recorded (Fig. S1). The spectra obtained were corrected from the contribution of the buffer.

The fluorescence spectra were fitted using a five parameter weibull function (from software Sigma Plot 5.0) to determine the wavelength corresponding to the highest fluorescence intensity (λmax). The unfolding curves were analyzed on the basis of a two-state model (N ⇌ U) according to Dumoulin *et al.* (Dumoulin et al., 2002). This model is based on the assumption that the difference in free energy $\Delta G_{NU}^{\circ}(H_2O)$ between folded (N) and unfolded (U) states is linearly dependent on the GdmCl concentration.

The transition curves were therefore analyzed according to the following equation (Equation 1). (Dumoulin et al., 2002)

$$y_{obs} = \frac{y_N + p[GdmCl] + (y_U + q[GdmCl]\exp(-a)}{1+\exp(-a)} \; with\; a = \frac{\Delta G^{\circ}_{NU}(H_2O) - m_{NU}[GdmCl]}{RT}$$

$\mathbf{y_{obs}}$ is the measured λmax at a given GdmCl concentration, y_N and y_U are the values of λmax in the absence of denaturant for the native and denatured states, respectively. $\mathbf{\Delta G^{\circ}_{NU}(H_2O)}$ is the difference in free energy between N and U in the absence of denaturant. ***m*** is the measure of the dependence of the free energy on the GdmCl concentration. [GdmCl] is the GdmCl concentration. ***p*** and ***q*** are the slopes of the pre- and post-transition baselines, respectively. ***R*** is the gas constant and **T** the absolute temperature.

The midpoints of the transition, i.e., the GdmCl concentration, at which [U]/[N] is equal to 1, is given by the following equation (Equation 2):

$$Cm = \frac{\Delta G^{\circ}(H2O)}{m}$$

2.3.2. Fluorescence spectroscopy

All fluorescence measurements were carried out using a Cary Eclipse fluorescence spectrophotometer (Varian, Palo Alto, CA, USA) equipped with a 4-cells Peltier cell-holder and 1 cm path length quartz cells. The intrinsic fluorescence emission spectra were recorded at 25°C using the following parameters: 295 nm excitation wavelength, emission spectra were recorded between 305 nm and 460 nm. Both excitation and emission slid width were 5 nm, high voltage on the PTM was set at 750 V. The scan rate was 600 nm/min. For each sample, five spectra were accumulated, averaged, and corrected from the signal recorded for the buffer alone.

2.4. Stability of rhDNase and PEG30-rhDNase in ethanol

The stability of rhDNase and PEG30-rhDNase in ethanol was assessed at 4°C and 37°C. rhDNase or PEG30-rhDNase were incubated at a concentration of 0.4 mg/ml (without counting the PEG mass in the concentration) in 150 mM NaCl, 1 mM $CaCl_2$ with 10% (v/v) or 50% (v/v) ethanol. Solutions of rhDNase or PEG30-rhDNase in 150 mM NaCl, 1 mM $CaCl_2$ kept at 4°C were used as controls. At regular time points, aliquots were sampled, and the stability was evaluated by quantifying non-soluble and soluble aggregates by UV spectrophotometer and size exclusion chromatography (SEC), respectively. For this, UV spectra (220 nm to 360 nm) were recorded before and after centrifugation 10,000 g for 10 min to assess the presence of non-soluble aggregates. Soluble aggregates as well as potential degradation products were investigated by injecting the supernatants into analytical SEC column (Increase 10/300 GL column, Cytiva, Belgium). Elution was monitored at 280 nm and/or 215 nm. In addition, the enzymatic activity of rhDNase and PEG30-rhDNase was assessed at different intervals by the methyl green assay.

2.5. Enzymatic activity by the methyl green assay

The activity of rhDNase and its PEGylated forms was assessed using the methyl green (MG) assay described elsewhere (Guichard et al., 2017, Sinicropi et al., 1994). The MG assay relies on the ability of deoxyribonucleases to hydrolyse DNA-methyl green substrate (DNA-MG) and release free MG which becomes colourless leading to a decreased optical density (OD) over time. Samples were initially diluted to a nominal concentration of 5.4 nM (200 ng/ml rhDNase) followed by serial dilutions on 96-well plate then DNA-MG solution was added to all wells. Plates were sealed and incubated in a humid chamber at 37°C for 24 h and OD was measured at 620 nm by SpectraMax i3 (Molecular Devices, CA, USA).

2.6. Viscosity of rhDNase and PEG30-rhDNase solution

Rheology assays were performed using the rheometer MCR102 at 20°C. 350 µl of rhDNase or PEG30-rhDNase solutions in standard storage buffer (150 mM NaCl, 1 mM $CaCl_2$) were loaded on the rheometer using a parallel plate of 50 mm of diameter (PP50) and a gap of 0.1 mm. Measurements were conducted at constant shear rate of 100 s-1 or 200 s-1 for 60 seconds (3s interval) and data were acquired by RheoCompass™ software. Experiments were performed in triplicate. Average viscosity values were expressed in mPa.s.

2.7. Aerosol characterization

Three concentrations of PEG30-rhDNase (1, 3 and 5 mg/ml, without counting the PEG mass in the concentration) were nebulized using InnoSpire Go (8 ml medication reservoir, 1.5 ml loaded volume) or optimized eFlow device (4 ml medication reservoir, 1.0 ml loaded volume) equipped with different aerosol heads (class 30 or class 40HO). Similar eFlow Technology nebulizer configurations are available in the US, Canada, Europe and Japan. Nebulization output as well as particle size distribution of the generated aerosols were measured by laser diffraction on HELOS BR (Sympatec GmbH, Clausthal-Zellerfel, Germany) in combination with the INHALER 2000 set at an inhalation flow rate of 30 L/min (laboratory of Professor Erik Frijlink, University of Groningen). This flow rate was used to prevent overloading and recirculation in the central unit of the laser diffraction. Data acquisition was initiated once a stable aerosol cloud was produced by the nebulizer (i.e., after 10 seconds). Three repeated cycles consisting of 15 seconds nebulization followed by 10 seconds measuring were applied for each condition. The total nebulization time was 1 minute. The fine particle fraction (FPF) was defined as the cumulative fraction of particles with a size ≤ 5 µm in the particle size distribution collected by laser diffraction. The aerosol output was assessed by weighting the nebulizer before and after nebulization.

Aerosols generated at a constant flow rate of 30 L/min from different solutions of PEG30-rhDNase were collected in a Single Shot Impinger (a home-made impinger without any particle size cut-off) pre-filled with 2.5 ml storage buffer (150 mM NaCl, 1 mM $CaCl_2$) into which the aerosol was guided. Solutions left in the medication reservoir (cup) were also collected. All samples (from aerosols or cups) were transferred into a glass HPLC vial and stored at 4°C for further assessment by SEC and methyl green assay. The specific activity of nebulized protein was also calculated relative to the non-nebulized control. The aggregation and/or fragmentation of PEG30-rhDNase resulting from nebulization was monitored by SEC and reported as percent monomer species.

2.8. Statistics

Unless otherwise mentioned, all experiments were performed at least in triplicates and data are presented as mean ± SEM. ANOVA was used for multiple group comparisons and t-test was used to compare the mean of two groups. All statistical inferences are based on a two-sided

significance level of * $p < 0.05$, ** $p < 0.01$, and *** $p < 0.001$ and were carried out using GraphPad Prism version 8.00 (GraphPad Software, La Jolla California USA). MG assay curves were fitted using Four Parameter Logistic (4PL) Regression.

3. Results and Discussion

3.1. Thermodynamic stability of rhDNase and PEG-rhDNase

Previous work by our laboratory has shown that rhDNase conjugated to linear 20 kDa, linear 30 kDa or 2-armed 40 kDa PEG remained fully active after PEGylation (Guichard et al., 2021, Mahri et al., 2021). Yet, the effects of PEGylation on protein thermodynamic stability can either be positive (stabilization), negative (destabilization), or neutral (no effect) (García-Arellano et al., 2002, Rodríguez-Martínez et al., 2008, Rodríguez-Martínez et al., 2011, Jain and Ashbaugh, 2011, Plesner et al., 2011, Price et al., 2011, Liu et al., 2022). Therefore, it was important to assess whether PEGylation had an impact on the thermodynamic stability of rhDNase.

The thermodynamic stability of rhDNase and PEG-rhDNases was evaluated from GdmCl-induced unfolding transitions (Fig. 1). The thermodynamic stability data (Fig. 1 B) derived from intrinsic fluorescence analyses (Fig. 1A) showed that rhDNase is extremely stable to GdmCl denaturation with a $\Delta G^{\circ}_{NU}(H_2O)$ 94 ± 10 kJ/mol (mean ± SD) and an estimated Cm (GdmCl-concentration at the mid-point of the unfolding transition) of 2.7 ± 0.2 M. The conjugation of rhDNase to different PEGs significantly decreased its thermodynamic stability with $\Delta G^{\circ}_{NU\ (H2O)} < 45$ kJ/mol and Cm < 2.4 M. The highest molecular weight PEG (40 kDa) caused the largest shift of the unfolding transition to lower GdmCl concentrations (Fig. 1A).

Worth noting that GdmCl denaturation was largely irreversible, and PEG30-rhDNase gained back more enzymatic activity than rhDNase (Fig. S2). Thus, all the derived thermodynamic parameters are apparent parameters giving an estimation of the effects of PEGylation on the stability.

PEGylation significantly impacted the stability of rhDNase and the branched form of 40 kDa PEG seems to induce a higher destabilization to GdmCl than both linear 20 kDa and linear 30 kDa PEGs. As shown previously, PEGylation does not alter rhDNase secondary and tertiary structures, nor enzymatic activity (Guichard et al., 2017), and the destabilization it induces here on the tertiary structure only became apparent upon chemical stress. A destabilization upon PEGylation was observed by García-Arellano *et al.* and Sorret *et al.* (García-Arellano et al., 2002, Sorret et al., 2019) who reported a decreased thermodynamic stability of PEGylated Cytochrome C (5 kDa PEG) and recombinant human interleukin-1 receptor antagonist (rhIL-1ra) (20 kDa PEG), respectively. On the opposite Hadadian *et al.* demonstrated that PEGylated (10 kDa) human basic fibroblast growth factor (bFGF) showed higher stability to GdmCl-induced denaturation than its unconjugated form (Hadadian et al., 2015). bFGF was totally denatured when exposed to 0.8 M GdmCl whereas 10 kDa PEG-bFGF needed 1.2 M GdmCl to be denatured. Rodriguez-Martinez *et al.* showed that PEGylation of α-chymotrypsin with either 2 kDa or 5 kDa PEG stabilized the protein ($\Delta G^{\circ}_{NU(H2O)}$ increased from 25 to 45 kJ/mol) (Rodríguez-Martínez et al., 2008). Liu *et al.* have shown that the mono-PEGylation of alpha-1 antitrypsin with linear 30 kDa or 2-armed 40 kDa PEG on either the thiol group or the N-terminus did not alter the stability of the native protein under chemical and heat-induced denaturation (Liu et al., 2022). Note that $\Delta G^{\circ}NU(H2O)$ values of the native proteins just discussed above range from 16 to 39 kJ/mol. Even though the thermodynamic stability of PEG-rhDNases is decreased compared to that of rhDNase, rhDNase exhibits very high stability with a $\Delta G^{\circ}_{NU}(H2O)$ of ~94 kJ/mol and the stability of PEG-rhDNases still remains high (~40 kJ/mol) as compared to the stability of most other small monomeric proteins with $\Delta G_{NU}{}^{\circ}(H2O)$ typically in the range 20–60 kJ/mol (Goldenberg, 2021).

3.2. Stability in ethanol

Some literature suggests that rhDNase needs to be delivered to small airways for improved efficiency (Bakker et al., 2011, Bakker et al., 2014). Because electrospraying has the ability to generate very small aerosol droplets (~ 2 μm) with a very narrow size distribution (GSD < 1.4), unachievable with current mesh nebulizers (Ijsebaert et al., 2001), it was thought to be an ideal choice for delivering (PEG)-rhDNase to small airways in the lungs. To assess the suitability of our proteins to hydroelectrodynamic atomization, an innovative atomization technology under consideration, proteins must withstand the high concentrations of ethanol typically required for the proper functioning of electrospraying nebulizers.

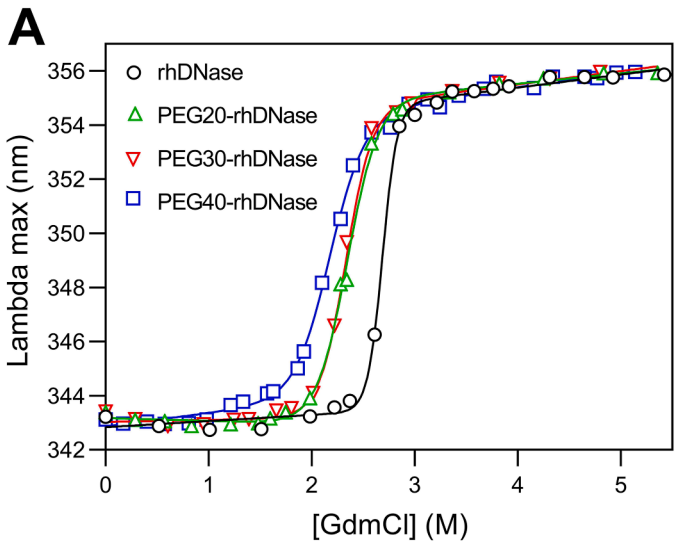

B

Protein	$\Delta G^{\circ}_{NU(H2O)}$ (kJ/mol)	m (kJ/mol·M)	Cm (M)
rhDNase	94 ± 10	35 ± 4	2.7 ± 0.2
PEG20-rhDNase	39 ± 4	17 ± 2	2.3 ± 0.2
PEG30-rhDNase	45 ± 3	19 ± 2	2.4 ± 0.2
PEG40-rhDNase	32 ± 2	15 ± 1	2.1 ± 0.1

Fig. 1. Thermodynamic stability of native and PEGylated rhDNase. A) GdmCl-induced unfolding transitions monitored by changes in the wavelength corresponding to the maximum fluorescence intensity (λmax). The protein concentration was 4.2 μM in 150 mM NaCl, 1 mM $CaCl_2$. B) Thermodynamic parameters (± standard deviation) derived from the GdmCl-induced unfolding of rhDNase and PEGylated rhDNases monitored by λmax. Cm, GdmCl-concentration at the mid-point of the unfolding transition. The transitions were analyzed based on a two-state (N↔U) model of denaturation. Note that, since the unfolding is not fully reversible, these parameters are apparent parameters.

Electrospraying was demonstrated to reproducibly generate aerosol particles with a narrow and tunable size distribution in the nano-micrometer range (Wang et al., 2019, Kavadiya and Biswas, 2018, Chen et al., 1995). Electrospraying have been investigated for several drugs by inhalation mainly by Battelle Pharma (Gomez, 2002) and recently by Gilbert Technologies; however, almost none for inhaled proteins. The few instances in the literature using electrospraying for therapeutic proteins were for drug delivery application other than inhalation (Wang et al., 2019, Moreira et al., 2021, Pareta et al., 2005).

PEG30-rhDNase was chosen as a reference PEG-rhDNase conjugate for ethanol compatibility studies since it has a relatively high thermodynamic stability [ΔG°_{NU} (H_2O) 45 ± 6 kJ/mol] and has shown good in vivo efficacy and safety profiles (Guichard et al., 2021). The stability of rhDNase and PEG30-rhDNase in terms of enzymatic activity and protein integrity was assessed in their storage buffer (150 mM NaCl, 1 mM $CaCl_2$) supplemented by ethanol concentrations up to 50% (v/v) both at +4°C and +37°C. Although high concentrations of ethanol (preferably higher than 85%) are commonly used for more efficient electrospraying, we did not go beyond 50% as a first step because of the known protein instability in organic solvents and because electrospraying can already function at these low ethanol concentrations (Pareta et al., 2005).

Results showed that rhDNase maintained its full activity at +4°C for 9 months regardless of the concentration of ethanol (Fig. 2 A.1). Note that commercial rhDNase, Pulmozyme®, has a shelf life of three years in

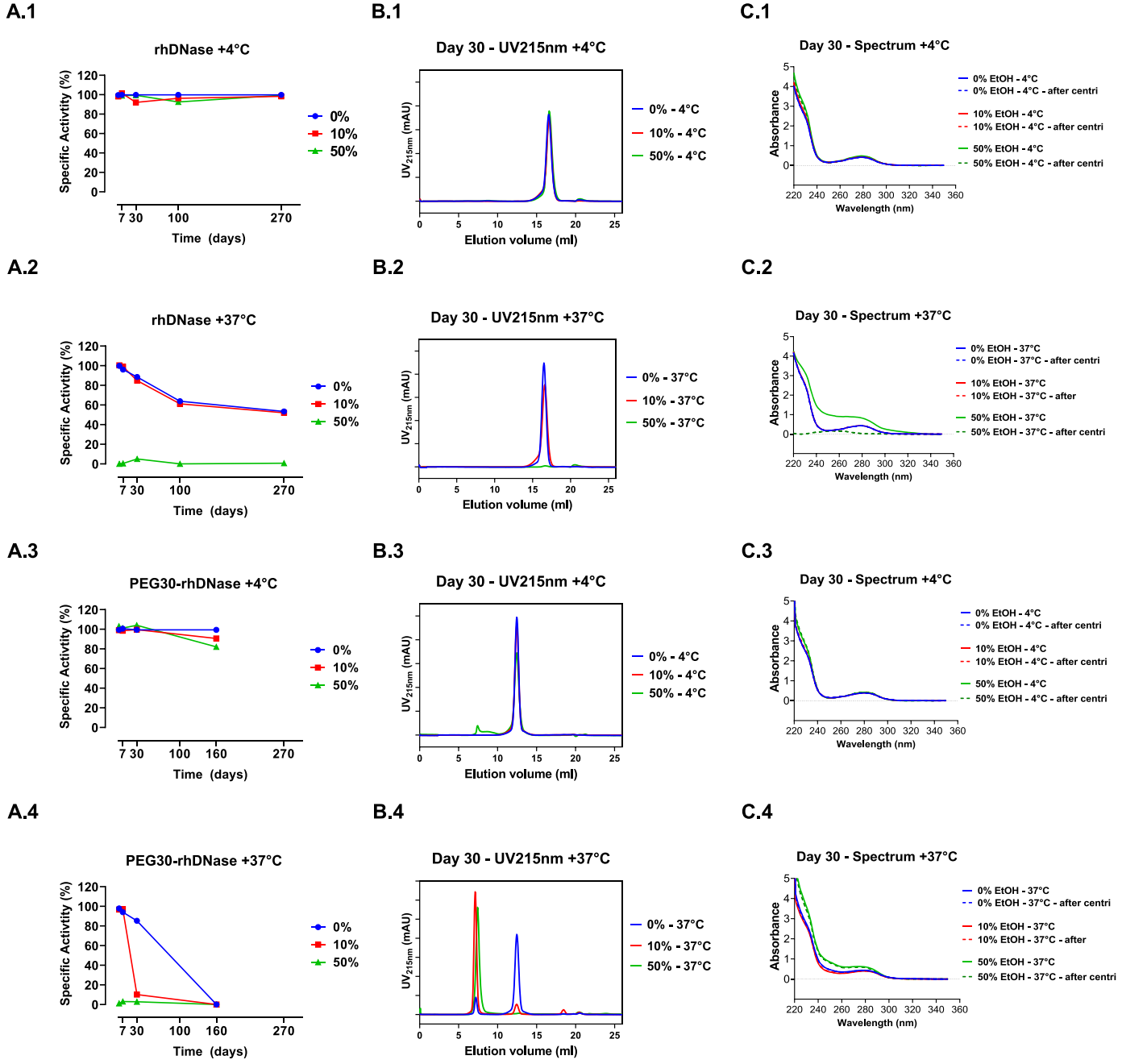

Fig. 2. Stability of rhDNase and PEG30-rhDNase in ethanol over time. Proteins were incubated at 0.4 mg/ml (without counting the PEG mass in the concentration) in 150 mM NaCl, 1 mM $CaCl_2$ supplemented with 10% or 50% ethanol (v/v). Ethanol was not added to the control (0% ethanol). Aliquots were taken at different time points and activity was assessed by methyl green assay (panel A). Representative SEC data (soluble aggregates) and UV spectrum measurements (non-soluble aggregates) at day 30 are presented in panel B and panel C respectively. Data for enzymatic activity are expressed as % specific activity, i.e., concentration of protein determined by activity assay divided by that based on UV absorption of the sample.

aqueous solution at 2-8°C. At 37°C, rhDNase suffered a total loss of activity within one day at 50% ethanol and about 40% loss after 100 days at 0% or 10% ethanol (Fig. 2 A.2). In contrast, PEG30-rhDNase was overall less stable compared with rhDNase at both +4°C and +37°C (Figs. 2 A.3 and A.4). At 4°C, PEG30-rhDNase suffered up to 20% loss of activity when stored in 10% and 50% ethanol at the 100-day mark (Fig. 2 A.3). Whereas, at 37°C, the activity loss was more significant compared with rhDNase at 0% or 10% of ethanol where a total loss of activity was observed after 160 days (Fig. 2 A.4). As rhDNase, PEG30-rhDNase suffered a total loss of activity within one day at 37°C in 50% ethanol.

In conjunction with the enzymatic activity data, SEC data showed that the rapid and total loss of activity at 37°C in 50% ethanol for both native and PEGylated rhDNase was associated with the presence of protein aggregates (Figs. 2 panel B and C and Figs. S3 and S4). While mainly non-soluble aggregates were observed for native rhDNase, soluble aggregates were dominant in the case of PEG30-rhDNase. The significant decrease in the UV absorption following centrifugation at 10,000 g for 10 min (Figs. 2 C.2 and Figure S3) along with the disappearance of the peak corresponding to the intact rhDNase from SEC (retention volume ca. 16.4 ml) confirms the presence of non-soluble aggregates (Figs. 2 B.2 and Fig. S3). Moreover, the appearance of small peaks eluting after the main peak of rhDNase may reflect the presence of degradation products especially when incubated in high concentrations of ethanol at 37°C (Fig. S3).

Remarkably, the total loss of activity of PEG30-rhDNase in 50% ethanol was observed as early as 4h at 37°C (Fig. S4). This total loss of activity was associated with the appearance of aggregates eluting at earlier retention volumes (ca. 7.54 ml) than the main peak of intact PEG30-rhDNase without significant decrease in the UV absorption after centrifugation at 10,000 g for 10 min indicating the soluble nature of these aggregates (Fig. S4). In addition, the increased levels of soluble aggregates were accompanied by a decrease in PEG30-rhDNase peak by SEC which is also consistent with the decreased enzymatic activity in Figs. 2 A.4.

It is known that most proteins are unstable and have low solubility in most polar solvents (e.g., ethanol) other than water (Pace et al., 2004). However, the very high thermodynamic stability of rhDNase provided an incentive for conducting these tests. Indeed, rhDNase was stable in 50% ethanol, at least at +4°C, which could have been sufficient to carry on investigating electrospraying. However, PEG30-rhDNase was less stable in ethanol at both 4°C and 37°C. Because even higher concentrations of ethanol (> 85%) are commonly used in formulations to be nebulized by electrospraying, not to mention the additional stressful conditions during generation of aerosols, this technology was deemed not suitable for the current PEG30-rhDNase formulation.

3.3. Stability to mesh nebulization

rhDNase is daily delivered by inhalation to patients with CF. Nebulization exposes the protein drug to physical stresses which can lead to protein denaturation and aggregation. A loss of stability of protein drugs after nebulization may impact their safety and efficacy. It was therefore necessary to assess the stability of PEG30-rhDNase to nebulization by different devices, especially because PEG30-rhDNase appears to be less stable than rhDNase to chemical denaturant and organic solvent. Currently, vibrating membrane technology is the fastest and most efficient way for rhDNase (Pulmozyme®) administration in the clinics. Both jet nebulizers and the vibrating mesh nebulizer, Pari eFlow Rapid, are approved for the clinical administration of rhDNase. Vibrating membrane technology generates aerosols by using a microperforated membrane that vibrates at high frequency subjecting the liquid drug formulation to forces during extrusion through the holes (Fig. S5 A). Two devices were selected to assess the stability of PEG30-rhDNase: the optimized eFlow nebulizer (PARI Pharma) and the InnoSpire Go (Philips). In comparison to the general purpose eFlow®rapid device, a set of handsets with virtually no residual volume and with interchangeable aerosol heads is available for optimized eFlow nebulizers allowing output rate and droplet size fine-tuning depending on the drug formulation.

Aerosol particle size distribution as well as protein activity and aggregate formation upon mesh nebulization were investigated for PEG30-rhDNase. Note that PEG30-rhDNase has been shown to be stable to nebulization at 1 mg/ml using a conventional compressed air nebulizer, and so was the other two PEG-rhDNases (Guichard et al., 2021). Conventional air-jet nebulizer, the first device approved by the Food and Drug Administration for pulmonary delivery of rhDNase (Fuchs et al., 1994), notoriously, induces significantly aggressive stress conditions for proteins. In order to shorten the nebulization time, high protein concentrations were tested using mesh nebulization in spite of the increased propensity of proteins to aggregate at high concentrations. Because solutions with high viscosities (> 2.0 mPa.s) could be challenging to nebulize, the viscosities of drug formulations containing different concentrations of the active ingredient were measured.

For the same protein concentration, PEG30-rhDNase solutions have higher viscosities compared with rhDNase solutions (Fig. 3). The viscosity of rhDNase and PEG30-rhDNase formulations increased with protein concentration but remained below 2.0 mPa.s (0.95 mPa.s and 1.53 mPa.s for rhDNase and PEG30-rhDNase, respectively, at 5 mg/ml). It is worth mentioning that nebulization of Ig-formulations with viscosities exceeding 3.5 mPa.s was successfully achieved using eFlow devices without any issues (Vonarburg et al., 2019). Based on solution viscosities, concentrations up to 5 mg/ml PEG30-rhDNase were considered suitable for nebulization testing using the eFlow devices and InnoSpire Go devices.

3.3.1. Optimized eFlow nebulizers

Several optimized eFlow handsets equipped with different aerosol heads (e.g. class 30, 35, 40 and 40HO), aerosol chambers (small, large, and extra-large) and medication reservoirs (1, 4 and 8 ml) exist (Fig. S5 A&B). Precision laser-drilled holes of different specific sizes allow droplet sizes adjustment from 2.5 μm to 5 μm. Based on our study objectives, the following configuration was chosen to be tested for PEG30-rhDNase (i) medication reservoir of 4 ml (ii) large aerosol chamber, and (iii) two aerosol heads – class 30 and class 40HO – that are interchangeable. Aerosol heads of class 30 produce the smallest aerosol droplets with the lowest output rate, while class 40HO aerosol heads produce the biggest droplets with the highest output rate and shortest nebulization time.

The size distributions of the aerosols generated by the optimized eFlow nebulizers were determined using laser diffraction, and the results are presented in Table 1. It is important to acknowledge that while laser diffraction provides rapid size-distribution measurements for homogeneous solutions, cascade impaction is the recommended method according to established guidelines (Preparation for nebulisation 2012). Compared to rhDNase nebulized with the traditional eFlow rapid device (Scherer et al., 2011), PEG30-rhDNase nebulized with the new eFlow devices had a lower volume median diameter (VMD) (< 3.02 vs 3.90 μm) ($p < 0.05$) and a higher fine particle fraction (FPF) (> 76% vs 72%) ($p < 0.05$), however, with a higher geometric standard deviation (GSD) for both Class 30 and Class 40HO aerosol heads (between 1.91 and 2.17 vs 1.57). Larger GSD reflects a wider size distribution curve, or in other terms, a less uniform particle size.

Comparing the results obtained with the class 30 and class 40HO aerosol heads, VMD values closely matched for all PEG30-rhDNase formulations. 40HO aerosol head resulted in higher GSD values ($p < 0.05$) and lower FPF (%) (only statistically significant for 1 and 3 mg/ml formulation, $p < 0.05$). As expected, the class 40HO aerosol head produced higher aerosol output rate compared with the class 30. Using both heads, the lowest aerosol output rates were registered for solutions of 5 mg/ml (0.72 ml/min and 1.19 ml/min for class 30 and 40HO, respectively). In absolute terms (mg/min), the higher the protein

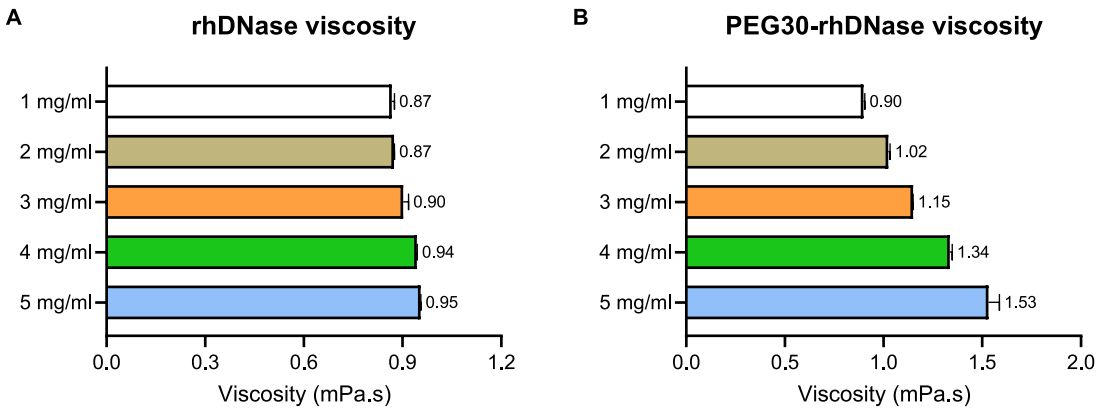

Fig. 3. Viscosity of formulations of rhDNase (A) or PEG-30-rhDNase (B) at protein concentration 1-5 mg/ml (without counting the mass of the PEG moeity in the concentration) in storage buffer (150 mM NaCl, 1 mM $CaCl_2$).

Table 1
Aerosol characteristics for rhDNase with the eFlow rapid compared to PEG30-rhDNase delivered by the optimized eFlow handset equipped with a vented medication reservoir cap (n=3).

Head	Concentration[1]	VMD (μm)[2]	GSD	FPF (%)[3]	Aerosol output (ml/min)	Estimated protein output (mg/min)
eFlow rapid (Scherer et al., 2011)	1 mg/ml	3.90 ± 0.20	1.57 ± 0.02	72 ± 3	/	/
Class 30	1 mg/ml	2.89 ± 0.05	1.91 ± 0.03	81 ± 1	1.04	1.04
	3 mg/ml	2.71 ± 0.09	1.97 ± 0.02	83 ± 2	0.76	2.28
	5 mg/ml	3.02 ± 0.05	1.96 ± 0.03	78 ± 1	0.72	3.6
Class 40HO	1 mg/ml	2.86 ± 0.13	2.09 ± 0.04	78 ± 2	1.41	1.41
	3 mg/ml	2.90 ± 0.06	2.17 ± 0.04	77 ± 1	1.51	4.53
	5 mg/ml	2.96 ± 0.05	2.13 ± 0.04	76 ± 1	1.19	5.95

Aerosol characterization was conducted by laser diffraction using breath simulation for rhDNase with the eFlow rapid (Scherer et al., 2011) and a constant airflow rate of 30 L/min for PEG30-rhDNase with the optimized eFlow

[1] The mass of the PEG moeity is not counted in the concentration.

[2] VMD (Volume Median Diameter) ≈ MMAD (Mass Median Aerodynamic Diameter) assuming density of our nebulized solution is 1 g/cm^3 and the form factor is spherical/equal to 1.

[3] FPF; fine particle fraction, the fraction of particles ≤5 μm.

concentration, the higher the estimated protein output rate. PEG30-rhDNase enzymatic activity and aggregate formation were assessed before and after nebulization by methyl green assay and SEC, respectively.

As can be seen in Table 2 & Fig. 4 and Fig. S6, PEG30-rhDNase collected from aerosols or remained in the medication reservoirs (cup) at the end of the nebulization cycle retained its enzymatic activity whatever the configuration (class 30 or 40HO) and tested concentration (1, 3 or 5 mg/ml). The absence of non-soluble protein aggregates was confirmed by absorbance measurement at 350 nm (zero absorbance) and 280 nm (there is no change) before and after centrifugation (10 000 g, 15 min, 4°C).

In summary, optimized eFlow devices can nebulize PEG30-rhDNase with similar or better aerodynamic properties than eFlow rapid device without compromising PEG30-rhDNase integrity or biologic activity. Moreover, by using several combinations concentration-aerosol head, the estimated absolute protein output was increased 5.7-fold: from 1.04 mg/min for 1 mg/ml-class 30 to 5.95 mg/min for 5mg/ml-class 40HO.

Table 2
Stability and activity of PEG30-rhDNase solution recovered from the medication reservoir (cup) and of PEG30-rhDNase aerosols after nebulization with the indicated eFlow configuration.

Head	Conc. (mg/ml)	Source	SEC (% monomer)	Protein conc. (mg/ml) #		Turbidity Abs_{350nm}	Activity relative non-nebulized control (%)
				Before	After		
Class 30	1	Cup	99.1	0.488	0.492	0.000	108 ± 6
		Aerosol	98.5	0.100	0.098	0.003	98 ± 11
	3	Cup	99.7	0.500	0.506	0.001	105 ± 6
		Aerosol	97.8	0.100	0.096	0.004	102 ± 12
	5	Cup	98.9	0.514	0.504	0,002	119 ± 13
		Aerosol	97.1	0.099	0.098	0.003	104 ± 12
Class 40HO	1	Cup	99.6	0.489	0.490	0.001	106 ± 13
		Aerosol	99.1	0.099	0.098	0.002	97 ± 8
	3	Cup	98.2	0.545	0.541	0.002	114 ± 16
		Aerosol	97.5	0.107	0.102	0.003	99 ± 18
	5	Cup	99,3	0.515	0.513	0.003	113 ± 10
		Aerosol	99.4	0.098	0.098	0.000	87 ± 5

The absence of activity loss for nebulized PEG30-rhDNase ('aerosol') relative to non-nebulized control was checked using a one-way ANOVA (Dunnett Multiple Comparison Test). # Protein concentration (without counting the PEG moiety) measurements by absorbance at 280 nm before and after centrifugation evaluating the presence of non-soluble aggregates. Samples of PEG30-rhDNase that were left in the medication reservoir after nebulization were diluted to 0.5 mg/ml (without counting the PEG moiety) in storage buffer and those collected from the aerosol were diluted to 0.1 mg/ml in storage buffer before subsequent analysis.

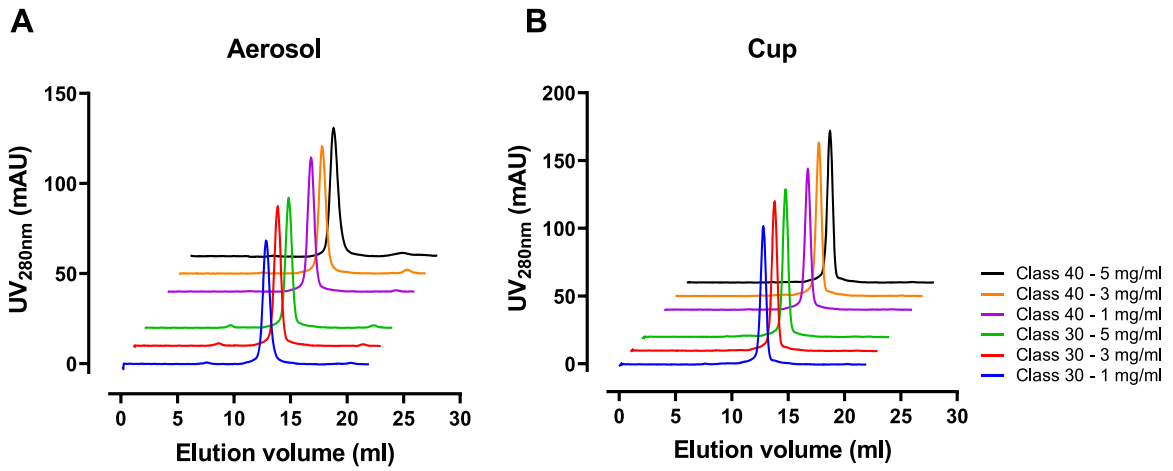

Fig. 4. SEC chromatograms of PEG30-rhDNase collected from aerosol (A) and cup (B) after nebulization using eFlow handsets equipped with class 30 and 40HO heads. PEG30-rhDNase concentrations were 1, 3, and 5 mg/ml in standard storage buffer (150 mM NaCl, 1 mM $CaCl_2$).

This improvement could bring the delivery time of a standard rhDNase unit dose of 2.5 mg under 30 seconds compared with 2-3 minutes for Pulmozyme® with the eFlow rapid device (Scherer et al., 2011). Despite the clear improvement over current nebulizers on the market, the real impact of this shorter delivery time on patients is difficult to predict as the delivered dose to the lungs is more complex as it is affected by different factors such as the patient age, disease stage, breathing pattern.

3.3.2. The InnoSpire Go

The InnoSpire Go is a small and silent hand-held nebulizer that only comes in a single configuration consisting of a vibrating mesh membrane and a medication reservoir (Fig. S5 C). Previous studies have shown that the InnoSpire Go generates an rhDNase aerosol cloud with an average droplet size (VMD) of 4.5 μm, a FPF (< 5 μm) of 55% and a span of 1.67 μm (Slator et al., 2017). It was therefore interesting to investigate how PEG30-rhDNase performed under this device.

Overall, the Innospire Go generated larger aerosol droplets and lower FPF than the optimized eFlow devices (Tables 1 & 3), which might not be optimal to reach small airways and treat the respiratory pathology in CF (Bakker et al., 2011). However, at higher protein concentration, the aerosol size was slightly smaller and the FPF higher, nevertheless without attaining the high FPF values of the eFlow.

Decreased aerosol output with increasing concentrations of PEG30-rhDNase was more significant for InnoSpire Go compared with the optimized eFlow devices. The aerosol output at 5 mg/ml was almost half that of 3 mg/ml resulting in an unexpected lower protein output for the former (1.15 mg/min vs 1.2 mg/min for 5 mg/ml and 3mg/ml, respectively). Regarding aerosol and protein output, the InnoSpire Go device was less efficient in delivering PEG30-rhDNase compared to the optimized eFlow devices, regardless of protein concentration and aerosol head.

Similar to the eFlow devices, PEG30-rhDNase exhibited high conformation resistance to nebulization by the InnoSpire Go device at different concentrations (1, 3, and 5 mg/ml) (Table 4 and Fig. 5). PEG30-rhDNase activity as well as integrity were overall maintained and were comparable to PEG30-rhDNase nebulized by the eFlow nebulizer device or control PEG30-rhDNase which did not undergo nebulization. SEC data showed a slight increase in the percentage of soluble aggregates mostly in the aerosol but not the medication reservoirs (cup) (Figs. 5A). Soluble aggregates were quantified based on the percentage surface area of the peak eluting at ca. 7.5 ml retention volume (Figs. 5B) before the main peak of monomer (ca. 12.7 ml). The relatively large peak apparent in the SEC chromatogram of InnoSpire Go cup at retention volume ca. 18.7 ml affected the total percentage of monomers of PEG30-rhDNase assessed at 1 mg/ml (90.6%), however, surprisingly, without significant impact on the enzymatic activity of PEG30-rhDNase. Absorption at 280 nm of both PEG30-rhDNase collected from both aerosols and cup did not show significant decrease after centrifugation (10 min at 10,000 g) indicating the absence of significant amount of insoluble protein aggregates.

In this study, soluble aggregates (primarily oligomers by SEC) and insoluble aggregates were investigated. However, it is important to acknowledge that our investigation did not specifically address other potential aggregate populations, such as submicronic aggregates. Even when no activity loss is detected, it is crucial to recognize that aggregates, irrespective of their impact on activity, may pose immunogenicity concerns, potentially compromising safety.

4. Conclusion

PEGylation with high molecular weight PEGs (20, 30 and 40 kDa) was shown to negatively affect the thermodynamic stability of rhDNase, with the largest conjugate, PEG40-rhDNase, being the least thermodynamically stable. The relative instability of PEG-rhDNases resulted in a less resistant PEG30-rhDNase to high ethanol concentrations compared with rhDNase, making hydroelectrodynamic atomization an off-the-table option for further development. On the bright side, the decreased stability did not affect the nebulization of PEG30-rhDNase

Table 3
Aerosol characteristics for rhDNase and PEG30-rhDNase delivered by the InnoSpire Go (n=3).

Protein	Concentration[1]	VMD (μm)[2]	GSD	FPF (%) [3]	Aerosol output (ml/min)	Estimated protein output (mg/min)
rhDNase (Slator et al., 2017)	1 mg/ml	4.5	/	55	/	/
PEG30-rhDNase	1 mg/ml	3.50 ± 0.02	2.04 ± 0.01	69.5 ± 0.3	0.55	0.55
	3 mg/ml	3.68 ± 0.06	1.94 ± 0.02	68 ± 1	0.40	1.20
	5 mg/ml	3.44 ± 0.14	1.95 ± 0.01	74 ± 3	0.23	1.15

Aerosol characterization was conducted by laser diffraction using a constant airflow rate of 15 L/min for rhDNase (Slator et al., 2017) and a constant airflow rate of 30 L/min for PEG30-rhDNase. [1]The mass of the PEG moeity is not counted in the concentration. [2]VMD (Volume Median Diameter) ≈ MMAD (Mass Median Aerodynamic Diameter) assuming density of our nebulized solution is 1 g/cm^3 and the form factor is spherical/equal to 1. [3]FPF; fine particle fraction, the fraction of particles ≤5 μm.

Table 4
Stability and activity of PEG30-rhDNase solution recovered from the medication reservoir (cup) and of PEG30-rhDNase aerosols after nebulization with the indicated eFlow configuration.

	Conc. mg/ml	Source	Soluble aggregates[1] (%)	% Monomers Relative to control	Protein conc. (mg/ml)[2] Before	After	Activity relative to control (%)
InnoSpire Go	1	Aerosol	1.73%	101.6%	0.133	0.144	121 ± 6
		Cup	0.00%	90.6%	0.100	0.105	95 ± 6
	3	Aerosol	0.78%	103.3%	0.105	0.112	115 ± 7
		Cup	0.00%	103.2%	0.100	0.098	104 ± 3
	5	Aerosol	0.84%	102.0%	0.110	0.114	104 ± 5
		Cup	0.00%	102.5%	0.099	0.107	124 ± 4[3]
Control	5	NA	**0.51%**	**100.0%**	0.155	0.154	100 ± 5

[1] Soluble aggregate percentage is calculated based on the surface area of peaks eluting before the main monomer peak relative to total surface area of peaks
[2] Protein concentration (without counting the mass of the PEG moiety) measurements by absorbance before and after centrifugation evaluating the presence of insoluble aggregates.
[3] No significant loss of activity for nebulized PEG30-rhDNase relative to non-nebulized control (one-way ANOVA, Dunnett Multiple Comparison Test ($p = 0.055$).

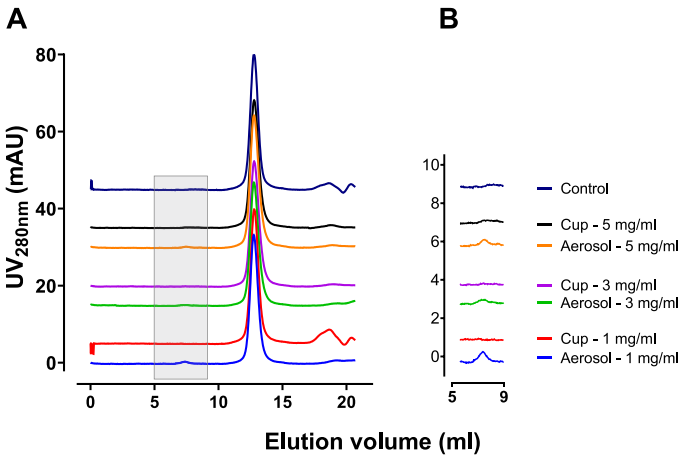

Fig. 5. SEC chromatograms of PEG30-rhDNase after nebulization by InnoSpire Go device. A shows full chromatograms and B highlights soluble aggregates eluting between 5-9 ml (grey area in A). PEG30-rhDNase solutions at 1,3, and 5 mg/ml (without counting the mass of the PEG moiety in the concentration) in standard storage buffer (150 mM NaCl, 1 mM CaCl2) were nebulized using InnoSpire Go. Aerosols and cups were collected and injected in Superose® 6 Increase 10/300 column. A solution of PEG30-rhDNase at 5 mg/ml that did not undergo nebulization was used a control.

with the InnoSpire Go and optimized eFlow devices, both using vibrating membrane technology. Both devices efficiently nebulize PEG30-rhDNase to generate aerosols with desirable particle size distribution and the fine particle fraction of the optimized eFlow nebulizer was higher compared with rhDNase nebulized with the eFlow rapid. Although nebulization behaviour did not depend on the PEG30-rhDNase concentration or aerosol head class of the optimized eFlow device, it was dependent on PEG30-rhDNase concentration with the InnoSpire Go with tiny aerosols and high FPFs only attained at the highest concentration tested. No significant integrity or enzymatic activity loss were recorded for PEG30-rhDNase. The high output rate achieved for the highest protein concentration tested (5 mg/ml) and the aerosol head class 40HO of the eFlow nebulizer allows the delivery of large amounts of PEG30-rhDNase in a short time (under 30 seconds). This work demonstrates the technical feasibility of employing vibrating membrane devices to deliver high amounts of PEG30-rhDNase by inhalation. Although highly promising, these results need to be validated by clinical studies before drawing any conclusions regarding the clinical safety and efficacy of these drug-device combinations for treating patients with CF.

Declaration of Competing Interest

No competing interest to declare.

Data availability

Data will be made available on request.

Acknowledgements

This work was supported by research grants from the First Spin-off program of the Belgian Walloon Region (Grant 1910026) and Laboratoires SMB (Brussels, Belgium). We thank PARI for providing the optimized eFlow nebulizer device. Mireille Dumoulin and Rita Vanbever are respectively Research Associate and Research Director of the Fonds National de la Recherche Scientifique (F.R.S.-FNRS, Belgium).

Supplementary materials

Supplementary material associated with this article can be found, in the online version, at doi:10.1016/j.ejps.2023.106522.

References

Bakker, E.M., et al., 2011. Improved treatment response to dornase alfa in cystic fibrosis patients using controlled inhalation. Eur. Respir. J. 38 (6), 1328–1335.
Bakker, E.M., et al., 2014. Small airway deposition of dornase alfa during exacerbations in cystic fibrosis; a randomized controlled clinical trial. Pediatr. Pulmonol. 49 (2), 154–161.
Bodier-Montagutelli, E., et al., 2018. Designing inhaled protein therapeutics for topical lung delivery: what are the next steps? Expert. Opin. Drug Deliv. 15 (8), 729–736.
Bodier-Montagutelli, E., et al., 2020. Protein stability during nebulization: Mind the collection step! Eur. J. Pharm. Biopharm. 152, 23–34.
Chen, D.R., Pui, D.Y.H., Kaufman, S.L., 1995. Electrospraying of conducting liquids for monodisperse aerosol generation in the 4 nm to 1.8 μm diameter range. J. Aerosol Sci. 26 (6), 963–977.
Cipolla, D., et al., 1994. Assessment of aerosol delivery systems for recombinant human deoxyribonuclease. STP Pharma Sci. 4, 50–62.
Dumoulin, M., et al., 2002. Single-domain antibody fragments with high conformational stability. Protein Sci. 11 (3), 500–515.
Ekladious, I., Colson, Y.L., Grinstaff, M.W., 2019. Polymer-drug conjugate therapeutics: advances, insights and prospects. Nat. Rev. Drug Discov. 18 (4), 273–294.
Fuchs, H.J., et al., 1994. Effect of aerosolized recombinant human DNase on exacerbations of respiratory symptoms and on pulmonary function in patients with cystic fibrosis. The Pulmozyme Study Group. N. Engl. J. Med. 331 (10), 637–642.
García-Arellano, H., et al., 2002. High temperature biocatalysis by chemically modified cytochrome C. Bioconjug. Chem. 13 (6), 1336–1344.
Goldenberg, D.P., 2021. Protein Folding | Protein Folding and Assembly☆. In: Jez, J. (Ed.), Encyclopedia of Biological Chemistry III (Third Edition). Elsevier: Oxford, pp. 105–115.
Gomez, A., 2002. The electrospray and its application to targeted drug inhalation. Respir. Care 47 (12), 1419–1431 discussion 1431-3.

Guichard, M.J., et al., 2017. Production and characterization of a PEGylated derivative of recombinant human deoxyribonuclease I for cystic fibrosis therapy. Int. J. Pharm. 524 (1-2), 159–167.
Guichard, M.J., et al., 2021. PEGylation of Recombinant Human Deoxyribonuclease I Provides a Long-Acting Version of the Mucolytic for Patients with Cystic Fibrosis. Adv. Therapeut. 4 (2), 2000146.
Hadadian, S., et al., 2015. Stability and biological activity evaluations of PEGylated human basic fibroblast growth factor. Adv. Biomed. Res. 4, 176.
Hertel, S.P., Winter, G., Friess, W., 2015. Protein stability in pulmonary drug delivery via nebulization. Adv. Drug. Deliv. Rev. 93, 79–94.
Ijsebaert, J.C., et al., 2001. Electro-hydrodynamic atomization of drug solutions for inhalation purposes. J. Appl. Physiol. (1985) 91 (6), 2735–2741.
Jain, A., Ashbaugh, H.S., 2011. Helix Stabilization of Poly(ethylene glycol)–Peptide Conjugates. Biomacromolecules 12 (7), 2729–2734.
Johnson, J.C., et al., 2008. Aerosol delivery of recombinant human DNase I: in vitro comparison of a vibrating-mesh nebulizer with a jet nebulizer. Respir. Care 53 (12), 1703–1708.
Kavadiya, S., Biswas, P., 2018. Electrospray deposition of biomolecules: Applications, challenges, and recommendations. J. Aerosol Sci. 125, 182–207.
Kettler, L.J., et al., 2002. Determinants of adherence in adults with cystic fibrosis. Thorax 57 (5), 459–464.
Liu, X., et al., 2022. Impact of the PEG length and PEGylation site on the structural, thermodynamic, thermal, and proteolytic stability of mono-PEGylated alpha-1 antitrypsin. Protein Sci. 31 (9), e4392.
Liu, X., et al., 2022. Production and characterization of mono-PEGylated alpha-1 antitrypsin for augmentation therapy. Int. J. Pharm. 612, 121355.
Lubamba, B., et al., 2012. Cystic fibrosis: insight into CFTR pathophysiology and pharmacotherapy. Clin. Biochem. 45 (15), 1132–1144.
Mahri, S., et al., 2021. Biodistribution and elimination pathways of PEGylated recombinant human deoxyribonuclease I after pulmonary delivery in mice. J. Control. Release 329, 1054–1065.
Mahri, S., et al., 2021. PEGylation of recombinant human deoxyribonuclease I decreases its transport across lung epithelial cells and uptake by macrophages. Int. J. Pharm. 593, 120107.
Moreira, A., et al., 2021. Protein encapsulation by electrospinning and electrospraying. J. Control. Release 329, 1172–1197.
Nasr, S.Z., et al., 2013. Adherence to dornase alfa treatment among commercially insured patients with cystic fibrosis. J. Med. Econ. 16 (6), 801–808.
Niven, R.W., et al., 1994. Protein nebulization: I. Stability of lactate dehydrogenase and recombinant granulocyte-colony stimulating factor to air-jet nebulization. Int. J. Pharma. 109, 17–26.
Niven, R.W., et al., 1995. Some factors associated with the ultrasonic nebulization of proteins. Pharm. Res. 12 (1), 53–59.
Niven, R.W., et al., 1996. Protein nebulization II. Stabilization of G-CSF to air-jet nebulization and the role of protectants. Int. J. Pharma. 127 (2), 191–201.
Nozaki, Y., 1972. The preparation of guanidine hydrochloride. Methods Enzymol. 26, 43–50.
Pace, C.N., et al., 2004. Protein structure, stability and solubility in water and other solvents. Philos. Trans. R. Soc. Lond. B Biol. Sci. 359, 1225–1234.
Pareta, R., et al., 2005. Electrohydrodynamic atomization of protein (bovine serum albumin). J. Mater. Sci. Mater. Med. 16 (10), 919–925.
Plesner, B., et al., 2011. Effects of PEG size on structure, function and stability of PEGylated BSA. Eur. J. Pharm. Biopharm. 79 (2), 399–405.
Preparation for nebulisation: Characterization, in 2.9.44, EuropeanPharmacopoeia, Editor. 2012.
Price, J.L., Powers, E.T., Kelly, J.W., 2011. N-PEGylation of a reverse turn is stabilizing in multiple sequence contexts, unlike N-GlcNAcylation. ACS Chem. Biol. 6 (11), 1188–1192.
Ratjen, F.A., 2009. Cystic fibrosis: pathogenesis and future treatment strategies. Respir. Care 54 (5), 595–605.
Respaud, R., et al., 2014. Effect of formulation on the stability and aerosol performance of a nebulized antibody. mAbs 6 (5), 1347–1355.
Respaud, R., et al., 2016. Development of a drug delivery system for efficient alveolar delivery of a neutralizing monoclonal antibody to treat pulmonary intoxication to ricin. J. Control. Release 234, 21–32.
Rodríguez-Martínez, J.A., et al., 2008. Stabilization of alpha-chymotrypsin upon PEGylation correlates with reduced structural dynamics. Biotechnol. Bioeng. 101 (6), 1142–1149.
Rodríguez-Martínez, J.A., Rivera-Rivera, I., Griebenow, K., 2011. Prevention of benzyl alcohol-induced aggregation of chymotrypsinogen by PEGylation. J. Pharm. Pharmacol. 63 (6), 800–805.
Rondon, A., et al., 2021. Protein Engineering Strategies for Improved Pharmacokinetics. Adv. Funct. Mater. 31 (44), 2101633.
Scherer, T., et al., 2011. A technical feasibility study of dornase alfa delivery with eFlow (R) vibrating membrane nebulizers: aerosol characteristics and physicochemical stability. J. Pharm. Sci. 100 (1), 98–109.
Sinicropi, D., et al., 1994. Colorimetric determination of DNase I activity with a DNA-methyl green substrate. Anal. Biochem. 222 (2), 351–358.
Slator, L., et al., 2017. Aerosol Particle Size Characterization of Several Common Respiratory Formulations from a Novel Handheld Mesh Nebulizer. Respiratory Drug Delivery Europe, Nice, France.
Sorret, L.L., et al., 2019. Steric Repulsion Forces Contributed by PEGylation of Interleukin-1 Receptor Antagonist Reduce Gelation and Aggregation at the Silicone Oil-Water Interface. J. Pharm. Sci. 108 (1), 162–172.
Suri, R., 2005. The use of human deoxyribonuclease (rhDNase) in the management of cystic fibrosis. BioDrugs 19 (3), 135–144.
Vonarburg, C., et al., 2019. Topical application of nebulized human IgG, IgA and IgAM in the lungs of rats and non-human primates. Respir. Res. 20 (1), 99.
Wang, J., Jansen, J.A., Yang, F., 2019. Electrospraying: Possibilities and Challenges of Engineering Carriers for Biomedical Applications—A Mini Review. Front. Chem. 7.